Proceedings of IMECE04
2004 International Mechanical Engineering Congress
Anaheim, California, USA, November 13-20, 2004

(DRAFT) IMECE2004-62117

DYNAMIC SIMULATION AND ANALYSIS OF A PASSIVELY SELF-STABILIZING HEXAPEDAL RUNNING ROBOT

Jonathan E. Clark
Mark R. Cutkosky
Department of Mechanical Engineering
Stanford University
Stanford, California 94305
Email: clarkj@cdr.stanford.edu

Darryl G. Thelen

Department of Mechanical Engineering
University of Wisconsin-Madison
Madison, WI 53706

ABSTRACT

The Sprawl family of robots have demonstrated that fast and robust locomotion is possible over uneven terrain with only feed-forward control. In the absence of feed-back, the speed, efficiency, and stability of the system are largely functions of how well the physical system is tuned. This work describes the development of a dynamic model used to investigate the effects of design changes on system stability and performance. Simulation results show the surprisingly large region of configurations that result in stable locomotion, and how the shape of this region changes as a function of the passive properties of the hips. Understanding of this is critical since peak performance, as measured by running speed, tends to occur on the boundary of stable configurations. Simulation results were used to quantitatively redesign the legs of a version of the robot configured to run outdoors. Implementation of the design changes resulted in doubling the robot's speed.

INTRODUCTION

With the construction of the *Sprawl* family of hexapedal running robots [1], we have demonstrated that a carefully designed mechanical structure can enable fast and stable locomotion over a variety of terrain without feed-back control. The tuning of the mechanical design, especially the compliant legs, has allowed the robots to run over hip-height obstacles at speeds of over 5 body-lengths per second ($0.8m/s$) .

With this approach, the emphasis is shifted from the design of the control system to the design of the structure of the robot. It therefore becomes increasingly important to understand the effect of varying design parameters on performance. Some parameters, such as actuation frequency and the nominal leg angles, are easily adjusted at run time. Others, such as the location of the center of mass, leg lengths, and hip flexure stiffnesses, require time-consuming design modifications. Nevertheless, it is critical for the designer to understand how these quantities affect the dynamics of locomotion.

We have used both simple and complex models to understand and refine the design of the *Sprawl* robots. The simplified models have consisted of spring-based, clock-driven hoppers derived from the pioneering work of Raibert and Koditschek [2,3]. Subsequent investigations of open-loop vertical hopping [4–6] have provided important insights regarding thrust timing, ground contact, hop height and stability. However, the real robots reveal other behaviors that cannot be captured by such idealized models.

Our complex models consist of multi-body dynamic simulations of the running platform that include design parameters describing the system's geometry, mechanical characteristics and actuation. Other investigators have used similar approaches to design control systems for complex, multi-legged robots [7–9].

The work described in this paper is close in spirit to these efforts but is particularly concerned with determining the space of design parameters that will lead to fast, stable hexapedal locomotion with open-loop actuation.

In the following sections we describe the dynamic model

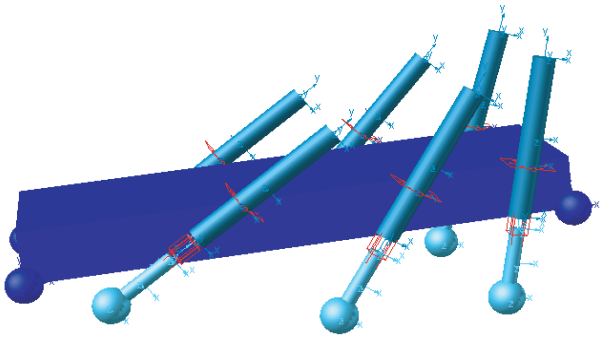

Figure 1. OVERVIEW OF SIMULATION OF SPRAWLITA FEATURING LEGS WITH PASSIVELY COMPLIANT HIPS AND PNEUMATICALLY ACTUATED THRUSTING LEGS

and the process of calibrating it with respect to the measured behavior of the *Sprawl* hexapods. Critical parameters of the model are then evaluated to determine the range of acceptable values that result in stable motion. This exploration of the parameter space indicates that there is a large set of configurations that result in stable running. Particular interest is paid to the passive stabilization and stance geometry parameters.

We also give an example of predictive power of the model, in which a version of our robot is redesigned and configured according to predictions of the model. The redesigned robot was able to run at more than double its previous speed while maintaining stability.

We conclude by illustrating the relationship between stance geometry and hip impedance in defining the range of leg configurations that result in fast and stable locomotion. We show that optimal performance is often found when the robot is configured to run on the boundary of stable operation. The simulation results also suggest that using the front and rear legs differently (introducing a for-aft sprawl angle) tends to increase the width of the stable configuration space.

MODELING AND SYSTEM IDENTIFICATION

Due to the complexity of the model that is required to investigate these issues, we chose to use the *MSC.ADAMS*^{TM} commercial dynamic simulation package as the modeling environment. *ADAMS*^{TM} offers an appropriate combination of integrator accuracy and stability, ease of building and parameterizing a design, and convenient display and analysis tools.

Care was taken to establish the parameters defining the passive self-stabilizing structure of the robot. As shown in fig. 1 the robot has an essentially rigid body supported by six identical legs. The center of mass of the robot is located slightly behind the middle legs, as in many insects [10] and as shown by Schmitt et al. [11] to promote lateral stability. Each leg has one active and one passive degree of freedom: a prismatic pneumatic actuator thrusts along the axis of the leg and a flexure provides rotational stiffness and damping at the hip where the leg attaches to the body. The robot also has servo motors at the hips, but these are used only to establish the equilibrium positions of the legs. Thus, as in insects, propulsion is due mainly to thrust forces directed along the legs, with elastic hip rotations being responsible for swinging the legs forward at the end of each stride. Each foot, as well as the corners of the body, has a contact model for collisions with the floor, and can drag and bounce. The various subsystems, and the system identification processes used in their development, are described in the following sections.

Legs - passive rotational elements

Each leg, as shown in fig. 2a, is fabricated using a technique called Shape Deposition Manufacturing (SDM) [12,13], and consists of two different grades of urethane. The clear structural material is approximately 13 times more rigid than the translucent white grade. The soft material was designed to act like the primarily passive tarsus-femur joint of a cockroach [14]. The flexure was designed so that the bending stiffness in the fore-aft and medio-lateral directions could be independently controlled by varying its dimensions.

The short length of the flexible section of the material compared to the length of the leg suggests modeling it as a small-length flexural pivot [15]. If one assumes that a pure moment is applied, then the rotation of a flexible beam can be described by the Bernoulli-Euler equation as $\Theta_0 = \frac{M_0\, l}{EI}$. Where M_0 is the applied moment, E is the modulus of elasticity of the bending material, and I is the mass moment of inertia of the flexure. For a Hookian spring described by $M_0 = K\Theta_0$ and a rectangular cross-sectional geometry (w,h) the stiffness K is simply:

$$K = \frac{E(wh^3)}{12\, l} \tag{1}$$

Based on the geometry of the flexures, the rotational stiffness should be 0.05 Nm in the fore-aft direction and 7.9 times stiffer (or 0.39 Nm) in the lateral direction. The effective spring constant in the fore-aft direction was measured experimentally and found to be 0.05 Nm. The softer, primary, mode of bending is in the direction of travel. Therefore, only a single degree of freedom was allowed in the initial version of the model. Later simulations indicated that during turning the lateral mode of bending becomes important. This addition, however, did not noticeably affect the straight-ahead motion of the simulation.

The urethane used in the leg flexures is viscoelastic and, as shown in [14], dissipates energy in a way not unlike that observed in cockroach legs. To simulate the observed energy loss

at running speeds, a viscous rotational damper was added in parallel to the hip spring on each leg. The effective damping was experimentally determined to be 2.3E-4 Nms.

The simulated response of the leg model to non-zero initial conditions was similar to the motion of the real leg as measured by high speed video. Figure 2b shows the results of a step disturbance for the robot leg as captured by high-speed video and the output from the ADAMS leg model. The thin solid line shows the average of several experimental step responses and dotted lines show the variability corresponding to one standard deviation. The heavy solid line is the simulated response, which produces similar energy dissipation for excursions corresponding to a standard step size, but faster decay for small excursions.

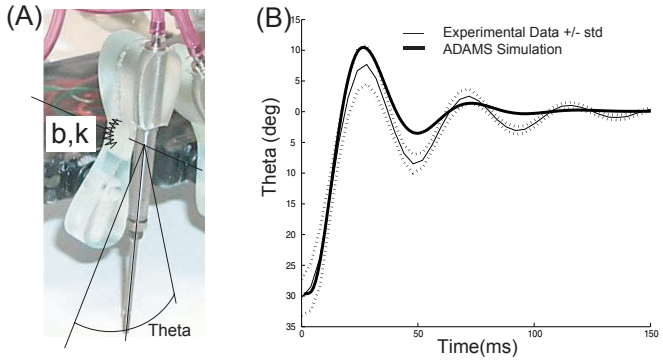

Figure 2. (A) OVERVIEW OF HIP MODEL AND (B) THE STEP DEFLECTION RESPONSE FOR BOTH THE ROBOT LEG AND THE MODEL

Table 1. FESTO PISTON VALUES

Festo Pistons	**Values**
Length	.058 m
Outer Diameter	.005 m
Inner Diameter	.004 m
Mass	.006 kg
Stiffness	55.0 N/m
Spring Preload	1.50 N
Damping	.002 Ns/m

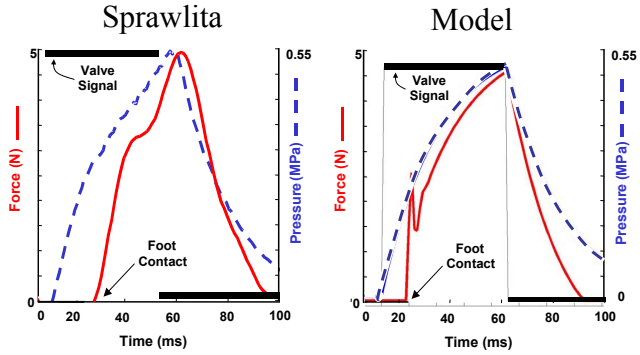

Figure 3. A COMPARISON OF THE PRESSURE RISE AND GROUND REACTION FORCE FOR THE ROBOT LEG AND THE MODEL

Legs - active translational elements

Each SDM leg has a spring-loaded, normally retracted, piston embedded in it (Fig. 2a). Consequently each leg is modeled with an active prismatic degree of freedom. The pistons are actuated by three-way pneumatic valves and the associated pressure rise and decay profiles are shown in Fig. 3a (dashed line).

The geometry, spring stiffness, and pre-load for the piston are all specified by the manufacturer and are given in Tab. 1. Note that these pistons have a 20mm stroke with hard stops at either end. The stops were modeled by stiff spring-dampers that engage at prismatic translations corresponding to the ends of the piston stroke.

The damping in the piston was modeled as pure viscus damping for simplicity. The value of the effective damping for the pistons was calculated experimentally, and is given in Tab. 1.

Each of the pneumatic valves is given a square wave signal as a control input. The frequency and duty cycle (% on) of the square wave determine the stride period and amount of thrust applied to the legs.

Tests have shown that the pressure rise in the robots is approximately exponential in nature, as shown in Fig. 3. Consequently, the first modeling efforts used a simple first-order ODE to calculate the pressure (p) acting on the piston:

$$\tau\dot{p}(t) + p(t) = p_0 \quad where\ p_0 = \begin{cases} p_{max} & \text{if valve on} \\ 0 & \text{if valve off} \end{cases} \qquad (2)$$

An advantage of this simple model is that it requires only a single parameter (τ) to characterize the pressure profile. A more complex model, accounting for the compressibility of the air and the orifice restriction at the valve, was introduced but did not significantly increase the overall accuracy of the locomotion simulations [16].

Contacts - Modeling (Robot/World Interaction)

During running, ground contact is intermittent and its initiation and duration are based on the open-loop clock timing, the piston pressure model, and the position and orientation of the body.

Foot/Ground Model Ground contact is always a challenging modeling problem and requires striking a balance between computational efficiency, numerical stability, and accuracy. The foot-floor contact in the vertical direction was modeled using a standard penalty method by the stiff nonlinear spring damper described in eq. 3.

$$F_n = k(x)^n + b\dot{x} \; for \; x > 0 \tag{3}$$

The ground characteristic parameters k, b, and n are the ground stiffness, damping, and exponential. These were experimentally measured for the foot and treadmill interaction and found to be 62,600 Nm, 10 Nm/s and 2, respectively.

The damping constant, b, ramps up from zero to full damping during a brief initial contact period in order to avoid numerical problems associated with discontinuous forces that can occur with intermittent contact. Horizontal foot forces were computed based on a Coulomb friction model. Static and dynamic friction coefficients were experimentally determined to be $\mu_s = 1.2$ and $\mu_d = 1.08$ for the rubber feet on the textured rubber treadmill. Friction coefficients also ramped up from zero to full friction over a brief initial contact period to avoid discontinuities in the horizontal forces.

The geometry of contact between the rounded feet on a flat treadmill was modeled as a sphere on a plane. This approximation allowed the use of an efficient closed-form model to compute the initiation of contact and depth of penetration between the feet and ground.

Body and Tether drag High speed video and simulations show that during normal running not only the feet, but also the rear of the robot makes contact with the ground. When running over obstacles, or when poorly configured, the front or 'nose' of the robot will at times also make contact with the ground. To account for this phenomenon, spherical contacts were added at the four lower corners of the box that represents the body of the robot (see Fig. 1). These contacts are treated in the same way as the foot contacts.

Although efforts were taken to minimize the size and weight of the connecting electrical cable, it still has a large impact on the running dynamics of the robot. It creates a drag force and affects the turning dynamics. The effect of these changes depends on how the tether is mounted and whether the robot is running on the treadmill or on the lab floor [17].

Initially no account was taken for the effect of the tether. This resulted in the model predicting speeds much higher than those demonstrated by the robot. The addition of a drag force, proportional to the filtered velocity of the robot and located at the center rear of the robot, accounts fairly well for the observed cable drag.

MODEL VERIFICATION

A comparison of the animation of the dynamic model versus high-speed video of the robot on a treadmill shows that the motions are quite similar, with nearly identical velocity, body orientation, actuator frequency, thrust duration, leg bend angles, and duration of airborne phases. [1]

Kinematic Comparison

A quantitative analysis of the difference between the robot and simulation was performed by comparing high-speed marker data from the robot running to simulation results. A summary of the numerical comparison of the kinematics is shown in table 2. As the table reveals, the leg flexing angles are quite similar despite omitting the angular drag due to the pneumatic tubing. In addition, the model runs somewhat more smoothly than the real robot with smaller vertical and angular motions of the body.

Table 2. KINEMATIC COMPARISON TABLE

Value per Stride	Model	Robot
ΔY Body COM	.0019 *m*	.0054 *m*
$\Delta\theta$ Front Legs	40.4 *deg*	35.6 *deg*
$\Delta\theta$ Middle Legs	30.6 *deg*	26.1 *deg*
$\Delta\theta$ Rear Legs	15.5 *deg*	14.4 *deg*
Δ Body Pitch	1.3 *deg*	2.9 *deg*
Mean Body Pitch	9.6 *deg*	8.8 *deg*

Parameter Sensitivity

For purposes of design, we are interested in the sensitivity of the running behavior to variations in the robot parameters. We

[1] The interested viewer can view a clip of the high-speed video (250 frames/second) superimposed on the animated model at the following URL: `http://dart.stanford.edu:88/Get/File-442/blend3_light.mov`.

have verified that the simulation is able to reproduce parameter sensitivities that we have observed experimentally. For example, the stride period used in the open-loop robot controller has a significant and non-linear effect on the speed of the robot [5]. As shown in Fig. 4, adjusting the stride period of the model has a similar effect on running speed and shows an optimum at the same period (approximately 130 ms) as observed for the robot. Thus the model should be useful for evaluating the effects of design changes when tuning the robot for speed. The curve for the model in Fig. 4 is consistently somewhat above that of real robot on a treadmill, due to imperfect modeling of the tether and ground friction. As discussed in the next section, if we tune the model to provide comparable ground reaction forces and tether force as measured for the robot, the model consistently runs faster but with the same sensitivity to stride period and leg angles.

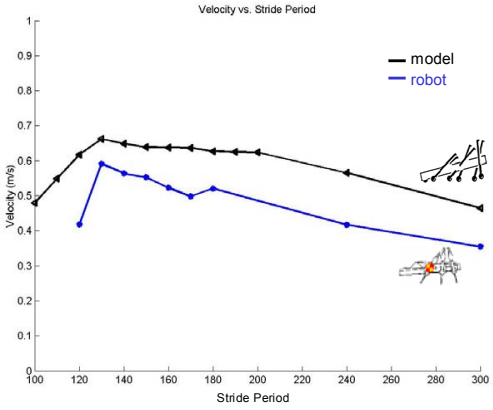

Figure 4. VELOCITY VS. STRIDE PERIOD FOR THE MODEL AND THE ROBOT

Ground Reaction Forces

Ground reaction forces dictate the acceleration of the body; hence verifying the accuracy of the ground forces predicted during a simulation is an essential test of the veracity of the model. The legs of the robot were designed to function like those of a cockroach, with the rear legs primarily propelling the robot forward, the front legs primarily braking at the end of each stride, and the middle legs performing both functions [1]. A comparison of the measured and simulated ground reactions demonstrates that the specialization of the legs is captured by the model (5). The model also correctly predicts the hind leg drag seen in the actual robot, which is an important aspect to consider when looking at ways to increase the speed.

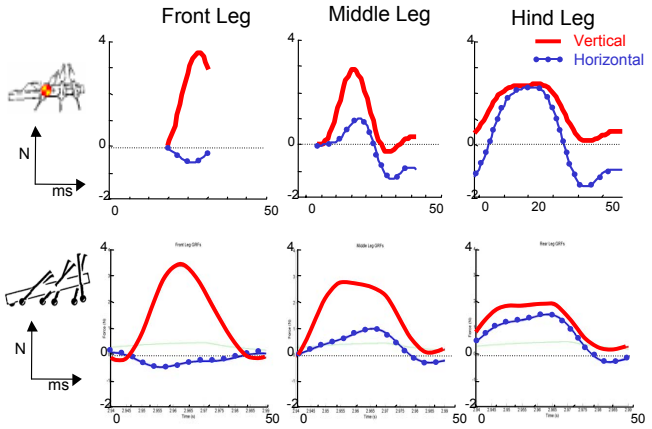

Figure 5. GROUND REACTION FORCES FOR EACH LEG OF THE ROBOT AND THE MODEL

APPLICATION OF MODEL IN DESIGN PROCESS

Up until the adaptations described in this report, all of the Sprawl family of hexapedal runners were confined to running indoors. Each platform was connected to an air supply and to a off-board microprocessor.

In order to free the robot from the lab, the microprocessor interface was replaced by onboard circuitry and a battery. Together these weighed about 100g (about 1/3 of the body mass) and were attached to the back of the Sprawl body. A portable air supply was provided by a small air tank that could be easily carried by the operator.

The difficulty with the implementation described above was that after adding the battery pack and a new set of stiffer legs the robot could only run at a top speed of less than 0.40 m/s. (As compared to the tethered versions that could run at speeds over 0.80 m/s.)

As a design exercise, the dynamic simulation was used to determine quantitatively what changes needed to be made to the robot in order to make its performance similar to its tethered cousins.

Approach

The simulation model was adapted to match the new robot's configuration by changing the valve pneumatics, adding mass for battery and six valves, and changing stiffness and damping of leg flexures. Parameter variation tests were then run to investigate the effect on the model of these changes.

Leg stiffness

Previous to the simulation studies the new robots hip flexures were initially scaled up from Sprawlita's 2.76 mm to 4.30 mm in order account for the larger mass of reconfigured robot. Our initial experiments with the simulation indicated that these

hips were probably too stiff. We therefore ran tests with stiffnesses from .05*Nm* (the value for *Sprawlita*) to .25*Nm* and evaluated the model's resultant forward velocity. For these tests hip damping was increased proportionally with stiffness.

Figure 6. EFFECT OF LEG HIP STIFFNESS ON VELOCITYFOR OUTDOOR SPRAWL

As shown in Fig. 6, there was a maximum with a hip stiffness of 0.094 Nm. Using eq. 1 we calculated the desired flexure width to be 3.1mm. We then modeled the step response of a leg with the predicted stiffness, damping, and inertia. For a leg with these properties, the maximum overshoot occurs at 55ms, which is the nominal duration of swing phase. It appears that as long as stability is preserved the legs operate best when tuned to oscillate at the robot's natural running frequency.

We then built legs with the calculated stiffness, and experimentally verified that the step response of the newly constructed leg corresponded well with the predicted profile.

Leg Orientation

With the revised leg design, we then tested the effect of changing leg orientations. To reduce the number of leg angle parameters we constrained contralateral pairs of legs to have the same orientation. We further constrained all 3 leg pairs such that the line of action of each piston intersected at a common point, as shown in Fig 7. With these constraints the orientation of all of the legs can be specified with two parameters. Plotting the location of this intersection point relative to the body of the robot allows for a geometric interpretation of the results.

Figure 7 shows the results of running the legs at 121 different settings chosen to span a reasonable region of the leg configuration space. The shaded region indicates the configurations for which the model 'nose dived' or crashed. For each stable configuration two circles are drawn, where the size of each circle is proportional to the minimum and maximum velocity at steady

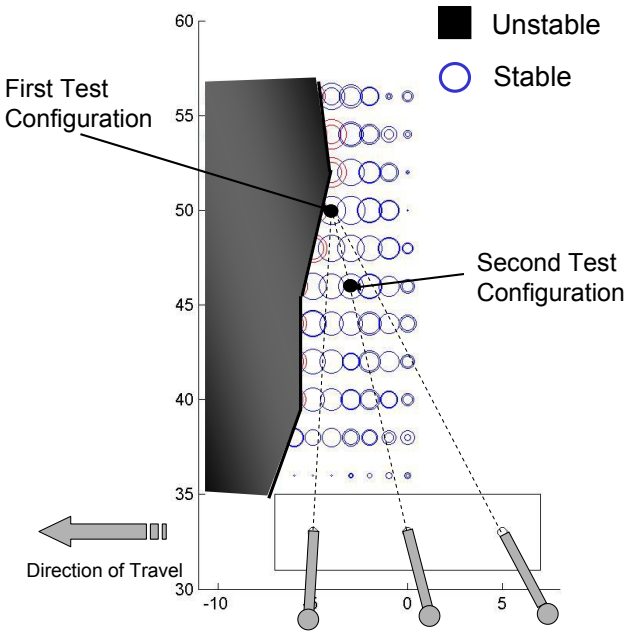

Figure 7. EFFECT OF LEG ANGLE ON VELOCITY FOR OUTDOOR SPRAWL. EACH GRID LOCATION REPRESENTS A DIFFERENT NOMINAL CONFIGURATION OF THE ROBOT. EACH POINT IS WHERE THE LINES OF ACTION OF THE LEGS INTERSECT. THE CIRCLE RADIUS AT EACH POINT IS PROPORTIONAL TO THE ROBOT VELOCITIES AT THAT CONFIGURATION. THE SHADED AREA REPRESENTS UNSTABLE OPERATION.

state. If two circles are visible, it is an indication of non-period-1 running.

The robot was tested at the initial configuration (as labeled on Fig. 7) which corresponds to the maximum predicted stable speed. The robot, however, tripped after a few strides due to small disturbances on the treadmill. Consequently, the second configuration (also labeled on Fig. 7) was chosen to increase stability while minimizing the loss in predicted speed. And, true to our predictions, the robot ran slightly slower, but much more stably.

Battery Pack Mass and Location

We also investigated the effect of varying the location and mass of the battery pack. Believing that these parameters were likely to be coupled, a simple design of experiments was used. Masses of 20, 60, and 100g and locations between 0.03 and -0.10 m (for and aft of the center of mass) were evaluated. We found that the coupling was, in fact, weak and that the added mass should be located at the robot's center of mass–suggesting that we have already identified the proper leg angles for balancing impulses. Increasing the mass from 20g to 100g monotoni-

cally decreased the speed by 0.20 m/s.

Results

After implementing the changes, the robot ran at 0.80m/s or well over twice as fast as before the changes were made. This demonstration highlights the utility of the simulation as a design tool.

TUNING THE SELF-STABILIZING POSTURE

In addition to suggesting specific design changes, the goal of the simulation is to give insight into how the robot runs, specifically how to tune the self-stabilizing leg structure. To this end more tests were run to look at the relationship between hip stiffness and leg angle. For this we varied the hip stiffness from 0.050 Nm to 0.250 Nm and evaluated the set of configurations that resulted in fast, stable running. As before, hip damping was also proportionally increased.

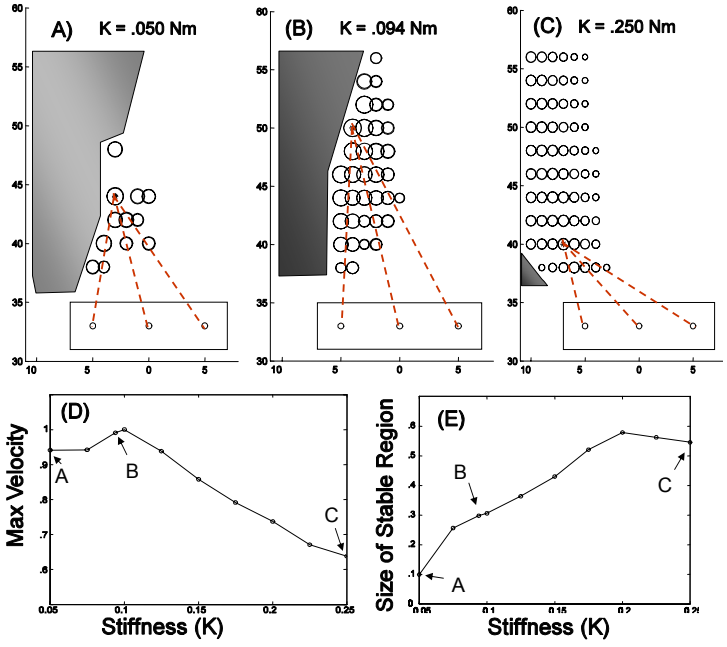

Figure 8. EFFECT OF ALTERING HIP STIFFNESS ON VELOCITY FOR A RANGE OF LEG ANGLES FOR: (A) THE SOFTEST HIPS TESTED, (B) OPTIMAL STIFFNESS SELECTED FOR OUTDOOR *SPRAWL*, AND (C) THE STIFFEST VALUE TESTED (D) SHOWS THE PEAK VELOCITY FOR ALL CONFIGURATIONS AT EACH LEVEL OF STIFFNESS TESTED. (E) SHOWS THE FRACTION OF TESTED CONFIGUATIONS AT EACH STIFFNESS THAT RESULTED IN FAST, PERIOD-1 RUNNING.

Figures 8(a-c) show the set of stable configurations for the minimum, newly selected optimal, and maximum stiffness. As in Fig. 7 the size of each circle is proportional to the model's velocity at that point. The shaded region on the left of each plot represents the unstable "nose diving" configurations. As the stiffness increases this boundary shifts and tilts forward relative to the body of the robot. The leg angles for the setting with maximum velocity are drawn as dashed lines. For the cases with the softer legs, this point occurs right on the boundary of stable configurations. This agrees with the prediction made by simple hopping models performed previously [6].

Figure 8(d) shows how the maximum velocity changes with stiffness. As the stiffness increases, each leg rotates less, shortening the stride length, which results in slower running. As shown in (a-c) above, as the hips get softer the leg angles have to shift to stabilize the robot. At the softest levels the front legs begin pointing backwards, resulting in negative work and slowing of the robot.

Figure 8(e) shows how the size of the stable region increases with hip stiffness. The size is calculated as the percentage of test configurations that result in fast and stable period-1 running. For large values of K, there is a remarkably large set of configurations that result in desirable running patterns. These values would be even higher for the largest hip stiffness if the test area were shifted to the left.

From Fig 8(a-c) we can see that, especially for comparatively soft legs, the postures that result in stable running are those where the orientation between the front and rear legs (or for-aft sprawl angle) is large (i.e. more sprawled). For a parallel leg orientation (as used by almost all multi-legged running robots) the intersection point would be at infinity. The simulation, however, indicates that as the legs become more parallel and the intersection point raises further above the body, the robot becomes less stable.

DISCUSSION OF RESULTS

The Sprawl robots employ an interesting form of locomotion. They trot and the employ an entirely passive leg swing. For a portion of the stride, they manifest quasistatic stability of the kind investigated in early robotic walking research (center of mass or pressure remains within the polygon of support [18–20]). However, they also have a brief airborne or pseudo flight phase (airborne with foot dragging). What keeps them from crashing is the timely repositioning of the swing legs before the robot falls too far forward. This, in turn, depends on leg stiffness (swing rate) and equilibrium angles of the legs (sprawl posture).

Therefore, there is a tradeoff among leg compliance, sprawl angle and leg thrusting that determines robot speed and open loop stability. Up to a point, if the leg hip flexures become softer, the stride length will increase, which leads to faster and more efficient locomotion (fewer actuator cycles per unit distance cov-

ered). However, when they get too soft, one of two constraints will be violated: (i) they may not swing into place in time for the given stride frequency – which leads to tripping, or (ii) as the leg excursions get larger the robot becomes less stable during stance in the sense of the traditional stability margins. This in turn, induces body rotations that lead to nose diving.

CONCLUSIONS AND FUTURE WORK

The robot simulation described in this paper was created with relative simplicity in order to highlight critical design parameters, while maintaining sufficient accuracy to predict the effects of changing those parameters. The simulation was successfully used to redesign and configure the robot with a significant (1/3 body mass) load.

More generally, the model has helped to verify the applicability of some of the findings of simple models to the robot. It has shown the importance of passively stabilizing leg elements, and indicates a need for further treatment of their effect on stability. It demonstrates that for the platform in question, increasing the hip stiffness, and to some degree the asymmetry or sprawl angle of the legs, increases range of configurations that result in stable running. This raises interest in the more general question of the role of leg asymmetry in running.

Future applications of the simulation include looking at the limits imposed on configuration and performance by friction, the role of fore-aft and lateral sprawl on the stability of a dynamic gait, the effect of environmental parameters on performance, and at adaptations schemes appropriate for various terrains.

The importance, and current lack of, good dynamic stability measures has also become clear from the simulations efforts described here. We need a better set of tools to evaluate dynamic stability for multi-legged bouncing robots, and to predict the ability of passive systems like Sprawlita to maintain balance in the face of large disturbances caused by rough terrain.

In conclusion, we have shown that detailed dynamic models can accurately predict the motion of running, hexapedal robots that use open loop thrusting actuation and passively swinging legs. Our simulation demonstrates that such models can be used to tune leg geometry, hip stiffness and stride period so as to produce stable, high speed locomotion using only open-loop control.

ACKNOWLEDGMENT

The authors would like to thank Arthur McClung, Sean Bailey, and all the folks at the BDML for their support. This work was supported by the Office of Naval Research under N00014-98-1-0669.

REFERENCES

[1] Clark, J. E., Cham, J. G., Bailey, S. A., Froehlich, E. M., Nahata, P. K., Full, R. J., and Cutkosky, M. R., 2001. “Biomimetic design and fabrication of a hexapedal running robot”. In Proceedings - IEEE International Conference on Robotics and Automation, vol. 4, pp. 3643–3649.

[2] Raibert, M. H., 1986. *Legged robots that balance*. MIT Press series in artificial intelligence. MIT Press, Cambridge, Mass.

[3] Kodistchek, D., and Buehler, M., 1991. “Analysis of a simplified hopping robot”. International Journal of Robotics Research, **10** (6) , pp. 587–605.

[4] Ringrose, R., 1997. “Self-stabilizing running”. In Proceedings - IEEE International Conference on Robotics and Automation, vol. 1, pp. 487–493.

[5] Cham, J. G., Karpick, J., Clark, J. E., and Cutkosky, M. R., 2001. “Stride period adaptation for a biomimetic running hexapod”. In International Symposium of Robotics Research.

[6] Cham, J. G., 2002. *On Stability and Performance in Open-loop Running*. PhD thesis, Stanford University.

[7] Saranli, U., Buehler, M., and Koditschek, D. E., 2000. “Design, modeling and preliminary control of a compliant hexapod robot”. In Proceedings - IEEE International Conference on Robotics and Automation, vol. 3, pp. 2589–2596.

[8] Klaassen, B., Linnemann, R., Spenneberg, D., and Kirchner, F., 2002. “Biomimetic walking robot scorpion: Control and modeling”. In Proceedings of the ASME Design Engineering Technical Conference, vol. 5, pp. 1105–1112.

[9] Osuka, K., Saruta, Y., and Kirihara, K., 2000. “Development and control of new legged robot quartet iii - from active walking to passive walking”. In IEEE International Conference on Intelligent Robots and Systems, vol. 2, pp. 991–995.

[10] Jindrich, D., and Full, R., 1999. “Many-legged maneuverability: Dynamics of turning in hexapods”. Journal of Experimental Biology, **202** (12) , pp. 1603–1623.

[11] Schmitt, J., and Holmes, P., 2000. “Mechanical models for insect locomotion: Dynamics and stability in the horizontal plane i. theory”. Biological Cybernetics, **83** (6) , pp. 501–515.

[12] Bailey, S. A., Cham, J. G., Cutkosky, M. R., and Full, R., 2000. “Biomimetic robotic mechanisms via shape deoposition manufacturing”. In International Symposium for Robitics Research (ISRR2000), J. Hollerbach and D. E. Koditschek, Eds.

[13] Merz, R., B., P. F., Ramaswami, K., Terk, M., and Weiss, L. E., 1994. “Shape deposition manufacturing”. In Proceedings of the Solid Freeform Fabrication Symposium.

[14] Xu, X., Cheng, W., Dudek, D., Hatanaka, M., Cutkosky, M. R., and Full, R., 2000. Material modeling for

shape deposition manufacturing of biomimetic componentsd, September 10-14.
[15] Howell, L. L., 2001. *Compliant Mechanisms*. Wiley, New York.
[16] Clark, J. E., 2004. *Design, Simulation, and Stability of a Hexapedal Running Robot*. PhD thesis, Stanford University.
[17] McClung, A. J., Cham, J. G., and Cutkosky, M. R., 2004. "Dynamic maneuvering of a biologically inspired hexapedal robot". In ASME IMECE Proceedings.
[18] McGhee, R. B., and Frank, A. A., 1968. "On the stability properties of quadruped creeping gaits". *Journal of Mathematical Biosciences,* **3** , pp. 331–351.
[19] Orin, D. E., 1976. *Interactive control of a six-legged vehicle with optimization of both stability and energy*. PhD thesis, The Ohio State University.
[20] Lin, B. S., and Song, S. M., 1993. "Dynamic modeling, stability and energy efficiency of a quadrupedal walking machine". In IEEE International Conference on Robotics and Automation, pp. 367–373.